

The Geometry of Continuous Latent Space Models for Network Data

Anna L. Smith, Dena M. Asta and Catherine A. Calder

Abstract. We review the class of continuous latent space (statistical) models for network data, paying particular attention to the role of the geometry of the latent space. In these models, the presence/absence of network dyadic ties are assumed to be conditionally independent given the dyads' unobserved positions in a latent space. In this way, these models provide a probabilistic framework for embedding network nodes in a continuous space equipped with a geometry that facilitates the description of dependence between random dyadic ties. Specifically, these models naturally capture homophilous tendencies and triadic clustering, among other common properties of observed networks. In addition to reviewing the literature on continuous latent space models from a geometric perspective, we highlight the important role the geometry of the latent space plays on properties of networks arising from these models via intuition and simulation. Finally, we discuss results from spectral graph theory that allow us to explore the role of the geometry of the latent space, independent of network size. We conclude with conjectures about how these results might be used to infer the appropriate latent space geometry from observed networks.

Key words and phrases: geometric curvature, graph Laplacian, latent variable, network model.

1. UNDERSTANDING NETWORK DATA THROUGH GEOMETRIC EMBEDDINGS

An important consideration in the development of an analytic strategy for understanding network data is the expected complexity of the types or patterns of connections in the network. In a statistical framework, we can formalize this notion through a particular dependence structure among the potential ties in the network. For example, a simple statistical model might treat each pair of nodes, or dyad, independently. Of course, this is typically not a reasonable assumption.

Anna L. Smith is a Postdoctoral Researcher at the Department of Statistics, Columbia University, 1255 Amsterdam Avenue, New York, New York 10027 (e-mail: als2356@columbia.edu). Dena M. Asta is an Assistant Professor at the Department of Statistics, The Ohio State University, 1958 Neil Avenue, Columbus, Ohio 43210 (e-mail: dasta@stat.osu.edu). Catherine A. Calder is a Professor at the Department of Statistics, The Ohio State University, 1958 Neil Avenue, Columbus, Ohio 43210 (e-mail: calder@stat.osu.edu).

tion. For example, in a social network, it is (at least heuristically) reasonable to assume that “the friend of my friend is also a friend of mine.” Indeed, this transitivity effect has strong theoretical support in the social network setting (Holland and Leinhardt, 1970) and has been observed in a variety of empirically observed networks as well. This expectation for complex non-dyadic dependence among nodes is not unique to social networks or the social sciences, but instead permeates network applications from various disciplines. However, note that such complex interactions directly contradict an assumption of dyad independence. If there is a connection between the i th and j th node and a connection between the j th and k th node, this tells us something about the probability of a connection between the i th and k th node.

This of course raises a natural question: What type of dependence is appropriate and how might this dependence affect an analysis of network data? One popular solution comes from the class of exponential random graph models (ERGMs). These models assume a particular dependence regime for the full set of potential ties in the network. In Frank and Strauss (1986)’s original formulation, Markov dependence is assumed (i.e., where all dyads that share a node are dependent), but more recent specifications have explored alternative dependence regimes (e.g. local conditional Markov dependence in Snijders et al., 2006).

Alternatively, we might consider representing this complex network data in an unobserved, latent lower-dimensional space and specifying a dependence regime there. This approach draws on ideas developed by (Lazarsfeld, Henry and Anderson, 1968) which proposed using latent variables to simplify complicated dependence structures and develop simpler model specifications: in these analyses, an unobserved latent variable is constructed such that the distribution of the data given the latent variables has a simple form. Of course, this idea has been utilized in a variety of settings, from factor analysis to item response theory to mixture models, and so it is no surprise that such a technique might be helpful in the network data setting. Additionally, we might consider choosing this lower dimensional space to be a metric space, in which case we are embedding the nodes of the network within a particular geometry. Although the details of the embedding may vary across applications or analytical methods, nodes’ positions in the latent space will correspond to features in the observed network with nodes that are connected in the network being closer together (or more generally, being more similar) in the latent space. That is, dependence in the network can be induced through distances, or similarities, between nodes in this lower-dimensional latent space. In practical settings, note that this framework provides a highly intuitive interpretation of the network data. For example, in the social network setting, we can interpret the embedding as a map of nodes’ relative positions in a latent “social space,” capturing the variety of unobserved social forces that may have influenced the observed pattern of social ties.

Traditionally, most latent space approaches have suggested embedding the nodes of the network in a Euclidean latent space. Although Euclidean space is certainly familiar and relatively easy to work with, it is not clear that it is the most appropriate geometry for network data or that Euclidean space is best equipped to reveal the variety of potentially interesting network features. More specifically, we argue that the geometry of the latent space plays an important role in determining both the fitness of the analysis for the particular observed

network data as well as the types of questions which the analysis is equipped to answer. In order to tease out this relationship, we will consider relating observed network features to latent space geometry through two different lenses: first, through common network summary statistics (e.g., transitivity and average degree) and second, through graph Laplacians which describe interesting features of networks and whose spectrum, under suitable assumptions of the latent space, is not influenced by network size.

We begin by summarizing existing approaches to the analysis of network data which take advantage of a lower-dimensional embedding of the nodes of the network in an unobserved latent space. In Section 2, we discuss commonly used similarity measures, focusing on methodology that is most amenable to the traditional statistical modeling framework. In Section 3.1, we review the variety of different types of latent spaces - from the familiar Euclidean space to more abstract spaces, like ultrametric space - in the continuous latent space model literature, in order to point out the impact the choice of geometry for the latent space can have on an analysis of network data. We argue that the geometry of the latent space can play an important role in understanding network data, highlighting the advantages of a newly proposed latent space for network data, hyperbolic space, in Section 3.2. In Section 4, we describe typical features of networks embedded in spaces with different curvatures using simulated network data. In this way, we connect the geometry of the latent space to features of networks that we typically care about, such as centralization measures and properties of the degree distribution. Finally in Section 5, we examine graph Laplacians to elucidate the relationship between the types of questions or discoveries that are possible in an analysis of network data which uses a latent space of a particular geometry.

2. CONTINUOUS LATENT SPACE MODELS FOR NETWORK DATA

A fully parametric model for network data provides a natural way to think about utilizing a lower-dimensional latent space for the nodes in the network. A generic form for such a model is given below:

$$(2.1) \quad \begin{aligned} Y_{ij} &\stackrel{ind}{\sim} \text{Bernoulli}(p_{ij}) & i \neq j; \quad i, j = 1, \dots, n \\ \text{logit}(p_{ij}) &= \alpha + s(z_i, z_j) \\ z_i &\in \mathcal{Z}^t, \quad z_i \stackrel{ind}{\sim} f_t(z|\psi) & i = 1, \dots, n, \end{aligned}$$

where Y_{ij} is a binary indicator of a tie between nodes i and j , z_i is the i th node's t -dimensional unobserved latent vector in the t -dimensional space \mathcal{Z}^t , and ψ parameterizes the distribution of the latent vectors in \mathcal{Z}^t . The generic latent space model assumes that network ties are conditionally independent, given the dyad's latent vectors. The probability of a tie depends on observed covariates as well as on some similarity measure, $s(\cdot, \cdot)$, of the latent vectors so that the probability of a tie is higher for nodes with similar latent vectors and lower for nodes with latent vectors that are dissimilar. In this sense, the latent vectors can represent the observed pattern of ties in the network as well as any unobserved attributes of the nodes that may have contributed to the pattern of observed ties. For example, in a social network, the latent vectors are typically interpreted as individuals' positions in a latent "social space," representing the variety of

unobserved social forces present in the observed network. In most cases, the similarity measure, $s(\cdot, \cdot)$, is chosen so that transitivity is a natural consequence of the model specification; if nodes i and j are tied (i.e., $s(z_i, z_j)$ is small) and nodes j and k are tied (i.e., $s(z_j, z_k)$ is small), then i and k are likely tied (i.e., $s(z_i, z_k)$ is likely small). This model can easily be generalized to incorporate homophily on observed attributes by simply adding a $\beta' x_{ij}$ term, where x_{ij} is a vector of (dyad-level) observed covariates for the dyad or pair formed by the i th and j th nodes. These latent space models typically require extra structure (e.g. hierarchical priors on the components of ψ) in order to model community structure and degree heterogeneity.

Here, we focus on methods that utilize a *continuous* latent space (CLS), although the use of a discrete space is also possible (e.g. the stochastic block models proposed by [Snijders and Nowicki, 1997](#), described briefly in Section 2.1). In practice, the dimension of the latent space, t , must be specified by the researcher, though traditional model selection techniques can be implemented to inform this choice. Without loss of generality, we will assume $t = 2$, which allows for easy visualization of the latent vectors and is a popular choice. Note that this model can be easily extended to networks with non-binary (i.e. weighted) ties using ideas from generalized linear models. Further, note that model 2.1 is written for directed ties, and subsumes the setting of networks with undirected ties by simply replacing the condition $i \neq j$ with $i < j$ (though this may have implications for the choice of $s(\cdot, \cdot)$). It is also worth pointing out that many existing network analysis methods which take advantage of a latent space representation do not require a fully parametric model, as outlined above, but instead fall under the umbrella of semi-parametric or non-parametric techniques. We will highlight this distinction in our discussion of these methods below.

In the rest of this section, we describe existing latent space models for network data in terms of their similarity measure, $s(z_i, z_j)$. In our discussion, we will group existing methods according to whether the proposed similarity measure has a dot product form, uses a distance metric, or is a graphon. However, these categories are not strictly distinct. For example, it may certainly be possible to rewrite a dot product model as a distance metric or perhaps to re-specify a distance model as a graphon. Further understanding of the connections between these models provides an interesting avenue for future research.

2.1 Dot Product Models

Many latent space methods for network data utilize a simple dot product similarity measure,

$$s(z_i, z_j) = z_i' z_j$$

In Euclidean space, the dot product measures the positioning of the vectors in the space. For vectors in \mathbb{R}^t , the dot product is related to both the angular distance, ϕ , and the Euclidean distance, $d(z_i, z_j)$, in the following ways:

$$\begin{aligned} z_i' z_j &= |z_i| |z_j| \cos \phi \\ &= \frac{1}{2} \left\{ |z_i|^2 + |z_j|^2 - [d(z_i, z_j)]^2 \right\}. \end{aligned}$$

The dot product in \mathbb{R}^t can be interpreted as the scaled cosine similarity (scaled by the magnitude of z_i and z_j) or equivalently as a function of the squared distance

Edge	Distance	Dot Product
$1 \leftrightarrow 4$	0.85 (1)	-3.34 (1)
$3 \leftrightarrow 5$	1.17 (2)	0.22 (8)
$1 \leftrightarrow 5$	1.31 (3)	-0.48 (5)
$1 \leftrightarrow 3$	1.45 (4)	-0.49 (4)
$4 \leftrightarrow 5$	1.86 (5)	-0.91 (2)
$2 \leftrightarrow 5$	2.11 (6)	-0.79 (3)
$3 \leftrightarrow 4$	2.28 (7)	-0.23 (6)
$1 \leftrightarrow 2$	3.16 (8)	0.90 (9)
$2 \leftrightarrow 3$	3.22 (9)	1.95 (10)
$2 \leftrightarrow 4$	3.24 (10)	-0.14 (7)

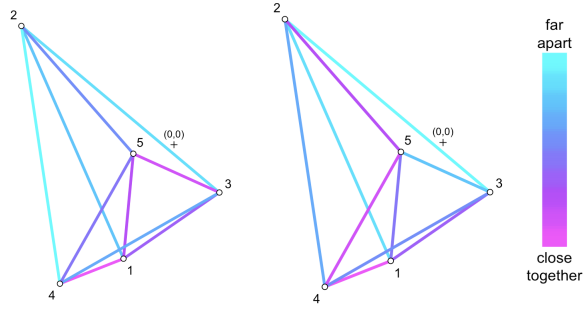


FIG 1. *Euclidean Distance and the Dot Product.* For illustration, five points are simulated from a standard bivariate normal distribution. In the network plots, edge color indicates the size of the similarity measure (Euclidean distance for the network on the left and dot product for the network on the right) between nodes, with magenta edges representing nodes that are least similar and cyan edges for those that are closest or most similar. Note that the ranking of similarities across the two networks is not identical, for example consider the edge between nodes 3 and 5.

between unit vectors in the direction of z_i and z_j . As can be seen in Figure 1, while the dot product in Euclidean space is certainly related to Euclidean distance, they are not equivalent measures. Although Euclidean distance is certainly much easier to visualize, the dot product is simpler to calculate and thus has computational benefits.

Most notably, the second version of the latent space model introduced in [Hoff, Raftery and Handcock \(2002\)](#), the so-called “projection model”, fits within this framework. [Hoff, Raftery and Handcock \(2002\)](#)’s projection model is specifically designed to handle directed network ties and is specified as follows:

$$(2.2) \quad s(z_i, z_j) = -a_i z_i' z_j \\ z_i \in t\text{-dimensional hypersphere},$$

where $a_i > 0$ is a sociality parameter for the i th individual. Note that $s(z_i, z_j)$ can be interpreted as the signed scalar projection of v_i onto v_j , where $v_i = a_i z_i$ and $v_j = a_j z_j$ are the scaled latent positions for the i th and j th node, scaled by their sociality parameters, a_i and a_j respectively (see Figure 2; note that the notation used here differs from that used in [Hoff, Raftery and Handcock, 2002](#)). The sociality parameters model a node’s tendency to send ties (i.e., to be “social”). Of course, the authors point out that this model could be easily adjusted to account for variability in nodes’ tendency to receive ties, by replacing a_i with a_j .

In practice, the authors suggest reparameterizing this model with alternative latent vectors, $v_i = a_i z_i$, so that

$$s(v_i, v_j) = \frac{v_i' v_j}{|v_j|} \\ v_i \in \mathbb{R}^t$$

This specification of the model is more parsimonious since it does not require a separate model for the sociality parameters. Further, since the v_i are now arbitrary positions in \mathbb{R}^t , we can simply choose $f_t(v|\psi)$ to be a standard Normal distribution, as the authors suggest for both versions of the latent space model proposed in [Hoff, Raftery and Handcock \(2002\)](#).

Other examples of dot product latent space models include [McCormick and Zheng \(2015\)](#)'s model for aggregated relational data (ARD) on the hypersphere (discussed in more detail in Section 3.1) and [Hoff \(2005\)](#)'s bilinear model, which incorporates additive node-level sociality effects to allow for degree heterogeneity,

$$\begin{aligned} s(z_i, z_j) &= a_i + b_j + z_i' z_j \\ a_i &\stackrel{iid}{\sim} \text{Normal}(0, \sigma_a^2), \quad b_i \stackrel{iid}{\sim} \text{Normal}(0, \sigma_b^2) \\ z_i &\stackrel{iid}{\sim} \text{Normal}(0, \sigma^2), \end{aligned}$$

where a_i and b_j are sociality effects for the i th and j th node respectively. [Hoff \(2005\)](#) motivates the interpretation of σ_a^2 , σ_b^2 , and σ^2 as random effects variances, highlighting similarities between the model and a traditional ANOVA model. In fact, these sociality effects inspired the similarity measures utilized in later models (e.g. [Krivitsky et al., 2009](#), see Section 3.1 for more discussion).

Dot product models in Euclidean space have been further developed by [Young and Scheinerman \(2007\)](#), [Nickel \(2007\)](#), and [Pao, Coppersmith and Priebe \(2011\)](#) as the class of random dot product graphs, where \mathcal{Z}^t is the $[0, 1]$ box in \mathbb{R}^t and $s(z_i, z_j)$ is the dot product, or some function of it.

We can also further generalize the type of similarity measure used in dot product models to a quadratic-like form,

$$(2.3) \quad s(z_i, z_j) = z_i' A z_j,$$

where A is a $t \times t$ -dimensional matrix. This specification subsumes the models discussed previously in this section, by simply choosing A to be the identity matrix. Examples include [Hoff \(2008\)](#)'s eigenmodel for undirected networks, [Hoff \(2009\)](#)'s SVD-inspired extension to directed networks, and [Minhas, Hoff and Ward \(2016\)](#)'s class of additive and multiplicative effects (AME) models.

It is also worth pointing out that the traditional stochastic block model (SBM) can be viewed as a special case of these quadratic-like latent space models. Generally, the stochastic block model assumes that the nodes can be separated into t unobserved latent classes where the membership vectors, z_i , are unknown. From model 2.1, assume $\beta = 0$ and let

$$\begin{aligned} s(z_i, z_j) &= p_{\pi(z_i), \pi(z_j)} \\ z_i &\sim \text{Multinomial}_t(1, \psi), \end{aligned}$$

where π maps nodes' latent vectors to t classes, $p_{t_1 t_2}$ parameterizes ties between nodes in the t_1 th and t_2 th classes, and ψ is a t -dimensional vector of membership probabilities. The model treats nodes within the same class as stochastically equivalent and parameterizes the probability of ties between nodes belonging to different classes by the $p_{t_1 t_2}$ s. Note that we can rewrite the similarity function in the quadratic-like form of equation 2.3 by letting A be a block-diagonal matrix of the $t(t + 1)/2$ -dimensional p vector. In the original versions of this model, the number of classes t was assumed to be known, though a variety of methods now exist to help understand the implication of different choices of t ([Saldana, Yu and Feng, 2015](#); [Chen and Lei, 2016](#)).

[Airoldi et al. \(2008\)](#) further extend this model by allowing nodes to have simultaneous partial memberships in each of the t classes in the mixed membership

stochastic block model (MMSBM) with

$$s(z_i, z_j) = z_i' A z_j \\ z_i \sim \text{Dirichlet}_t(\psi),$$

where again A is the block diagonal matrix of the between-class tie probability vector and ψ is a t -dimensional vector of membership probabilities. In this setting, the z_i s are still interpreted as unobserved latent membership vectors and further, can be viewed geometrically as positions on a $(t - 1)$ -dimensional simplex. In fact, in the original specification of the stochastic block model, the z_i can be viewed geometrically as the *vertices* of a $(t - 1)$ -dimensional simplex. In the MMSBM, the membership vectors have a geometric interpretation on the simplex: distance from a node's position on the simplex to a particular vertex (community) is an indication of how strongly that node's behavior in the network matches the behavior of the community as a whole.

2.2 Distance Models

A natural choice for $s(\cdot, \cdot)$ is a (negative) distance metric, in which case we can interpret the z_i s as latent positions in a t -dimensional latent metric space, \mathcal{Z}^t . We will refer to these special cases as latent distance models:

$$(2.4) \quad \begin{aligned} Y_{ij} &\stackrel{ind}{\sim} \text{Bernoulli}(p_{ij}) & i \neq j; \quad i, j = 1, \dots, n, \\ \text{logit}(p_{ij}) &= \alpha - d(z_i, z_j) \\ z_i &\in \mathcal{Z}^t, \quad z_i \stackrel{ind}{\sim} f_t(z|\psi) & i = 1, \dots, n, \end{aligned}$$

where d is the natural metric on \mathcal{Z}^t and f_t describes the distribution of latent positions in \mathcal{Z}^t . In a latent distance model, transitivity effects are guaranteed by the triangle inequality. Note also that these models are most appropriate for undirected ties, since distances are inherently symmetric. These models also allow us to visualize the nodes' latent positions by simply plotting estimates, \hat{z}_i , in \mathcal{Z}^t which can help illuminate previously unnoticed patterns in the data. For example, one could plot the latent positions from a null model and color the positions according to some covariate that could later be included in the model. Although this procedure is available to all versions of latent space models (whether distance is the chosen similarity measure or not), interpretation of relationships among nodes' latent positions in these plots is certainly more intuitive in the latent distance models.

Further, note that the concept of using distance to model dependence is not unique to the class of latent distance models for network data. In fact, this idea has had a long tradition of success in the statistical modeling literature. For example, in methods for continuous spatial data, distance is obviously a natural part of the modeling framework. Even in cases where spatial data is observed at an aggregate level (i.e., in some type of districts or areal units) the spatial weights matrix used in spatial regression models, such as CAR and SAR models, contains information about distance through a nearest neighbors matrix (where the ij th entry is one if the i th district neighbors the j th district and zero otherwise). In fact, in many spatial applications, non-Euclidean distances can be used to better represent the underlying dependence structure of the particular data generating process.

For example, a researcher might use stream or flow distance when considering chemical concentrations in a watershed area or perhaps travel time or travel cost for a group of city commuters. Further, models for phylogenetic data often make use of Hamming distance¹ to represent similarity among species when creating a phylogenetic tree. In short, using latent distances to model dependence among nodes in a network allows for an intuitive representation of an otherwise complex dependence structure and draws on the well-developed practices of using distance to model dependent data in other fields of statistical research.

Examples of latent space approaches which use distance include Hoff, Raftery and Handcock (2002); Handcock, Raftery and Tantrum (2007); Krivitsky et al. (2009) and will be discussed in more detail in Section 3.1.

2.3 Graphons

Graphons are a particular case of continuous latent space models where the latent space is uninteresting. To be precise, a graphon is essentially a measurable function $W : [0, 1]^2 \rightarrow [0, 1]$ symmetric in its coordinates (Lovász, 2012). In the general definition 2.1 of a CLS model, the z_i 's are uniformly drawn from $[0, 1]$ and $p_{ij} = W(z_i, z_j)$. Mixtures of graphons are exactly the distributions of infinite graphs invariant under permutations of the nodes (Lovász, 2012). Conversely, it is possible to formalize a sense in which a limit of suitable sequences of growing graphs uniquely identifies a graphon up to graphon equivalence (Diaconis and Janson, 2007).

While other CLS-based generative models typically fix the connection probabilities and vary the node densities, graphon-based generative models typically fix the node density (as the uniform distribution on $[0, 1]$) and vary the connection probabilities according to different W -functions. A graphon can be estimated by stochastic block models, or equivalently, the W -function can be estimated by certain piecewise constant functions $[0, 1]^2 \rightarrow [0, 1]$ (Airoldi, Costa and Chan, 2013; McMillan and Smith, 2016; Wolfe and Olhede, 2013; Yang, Han and Airoldi, 2014). It is difficult to constrain the class of W -functions based on salient network properties in order to improve the estimation process. In contrast, there exists a natural connection between the geometry of the latent space and salient network properties.

3. LATENT SPACE GEOMETRIES

In this section, we continue our description of continuous latent space models for network data, paying particular attention to the geometric properties of the latent space assumed under each model. In Section 3.1, we review existing approaches in Euclidean space (Section 3.1.1); elliptic space, such as the surface of a three-dimensional sphere (Section 3.1.2); and other spaces (Section 3.1.3). In Section 3.2, we highlight properties of hyperbolic space and detail its promising potential application in the class of continuous latent space models for network data, inspired by recent network analysis methods which take advantage of a hyperbolic latent space (Krioukov et al., 2010; Asta and Shalizi, 2014; Aldecoa, Orsini and Krioukov, 2015).

¹The Hamming distance between two vectors counts the number of positions at which the corresponding vectors differ.

3.1 Literature Review

3.1.1 *Euclidean Space* Perhaps the most intuitive specification of the latent space model is the Euclidean latent distance model, where \mathcal{Z}^t is the familiar t -dimensional Euclidean space and d is Euclidean distance,

$$\begin{aligned} d(z_i, z_j) &= |z_i - z_j| \\ &= \sqrt{(z_i - z_j)'(z_i - z_j)}. \end{aligned}$$

In fact, this version of the model was introduced by [Hoff, Raftery and Handcock \(2002\)](#) as the “distance model” and is certainly the most widely used latent space model for network data. The authors specify $f_t(z|\psi)$ as a standard normal distribution.

[Handcock, Raftery and Tantrum \(2007\)](#) extend this model to capture community structure in a network by letting $f_t(z|\psi)$ be a mixture of K multivariate normal distributions:

$$z_i \sim \sum_{k=1}^K \lambda_k \text{MVN}_t \left(\mu_k, \sigma_k^2 I_t \right),$$

where λ_k is the probability that a node belongs to the k th group ($\sum_{k=1}^K \lambda_k = 1$). Under this model, the latent positions are spatially clustered in \mathcal{Z}^t . Thus, this model can also be viewed as a generalization of the stochastic block model (see Section 3.1.3 for more details), with the k th mixture component representing the k th class, which also allows for transitivity within blocks and homophily on attributes. On the other hand, [Handcock, Raftery and Tantrum \(2007\)](#)’s model can be thought of as a restriction of [Hoff, Raftery and Handcock \(2002\)](#)’s version of the Euclidean latent distance model to better represent community structure in the observed network.

Although developed for directed ties, [Handcock, Raftery and Tantrum \(2007\)](#)’s model does not explicitly model degree heterogeneity. This extension is provided by [Krivitsky et al. \(2009\)](#) where the addition of additive individual random effects act as sociality or popularity effects to accommodate the differing tendency of nodes to send or receive ties, with

$$\begin{aligned} s(z_i, z_j) &= a_i + b_j - d(z_i, z_j) \\ a_i &\stackrel{iid}{\sim} \text{Normal}(0, \sigma_a^2), \quad b_i \stackrel{iid}{\sim} \text{Normal}(0, \sigma_b^2), \end{aligned}$$

where a_i is the sender effect for the i th node and b_j is the receiver effect for the j th node. The authors’ extension of [Handcock, Raftery and Tantrum \(2007\)](#)’s model borrows from the form of [Hoff \(2005\)](#)’s bilinear model, mentioned in Section 2.1. In both cases, the sender and receiver effects mimic the specification of an ANOVA model and can be interpreted similarly.

The latent Euclidean distance model has also been extended to the case of dynamic networks ([Sewell and Chen, 2015](#)).

While a Euclidean latent space certainly allows for easy visualization and interpretation of estimated latent positions and may be desirable given the familiarity with Euclidean geometry, it is not clear whether this geometry is best suited to represent the complex dependencies we typically encounter in network data. We will discuss this point further in Section 3.2.

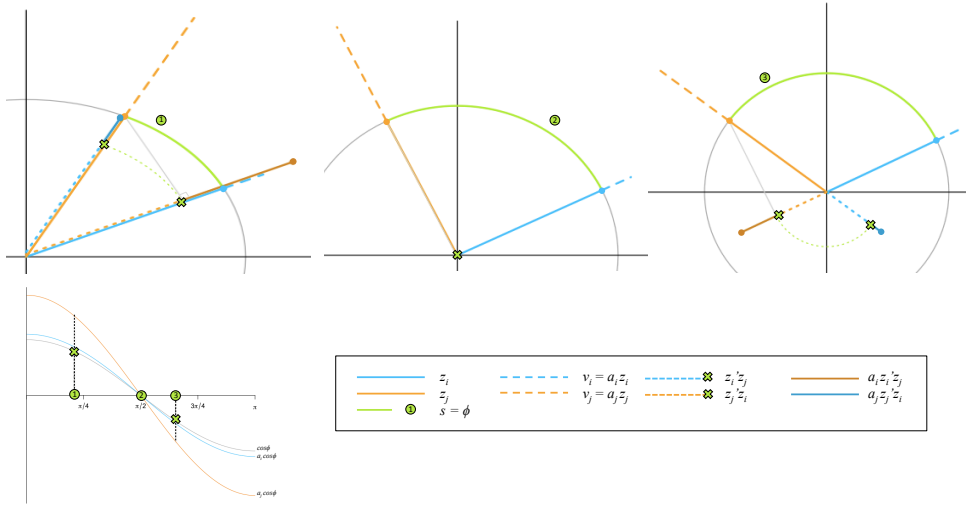


FIG 2. Visual interpretation of the choice of $s(\cdot, \cdot)$ in Hoff, Raftery and Handcock (2002)'s projection model, $t = 2$. Latent position vectors for the i th node are shown in blue and for the j th node are shown in orange. Across the top panel, we display three possible sets of latent positions, with their corresponding similarity measure in Hoff, Raftery and Handcock (2002)'s model displayed in the bottom left panel. Distance in this latent space, the unit hypersphere, is great circle distance or arc length and is displayed as green arcs in the top panels and green points in the bottom left panel.

3.1.2 The Unit Hypersphere As discussed in Section 2.1, Hoff, Raftery and Handcock (2002) introduces two versions of a latent space model: the distance model in Euclidean space (see Section 3.1.1) and the so-called projection model, which uses a dot product similarity measure and embeds nodes on the unit circle (i.e., a 1-dimensional unit hypersphere).

Note that this projection model is *not* an example of a latent distance model, since the natural distance metric on the hypersphere is great-circle distance (arc length). However, on the unit hypersphere, the great-circle distance between two latent positions, z_i and z_j , is equivalent to their angular distance, ϕ , and can be calculated as the inverse cosine of the dot product of z_i and z_j . Thus, the similarity measure in Hoff, Raftery and Handcock (2002)'s projection model (see Equation 2.2) is simply the *cosine similarity* between the latent position vectors, scaled by a sociality parameter, a_i . When z_i and z_j are close (and the angle between them is acute), $z'_i z_j$ will be positive and when they are far apart (and the angle between them is obtuse), $z'_i z_j$ will be negative. Thus, this choice of $s(\cdot, \cdot)$ preserves the relationship between the probability of a tie and some measure of “closeness.” That is, just as in the latent distance models, nodes that are “closer” together are more likely to be tied. Further, if this model were used for networks with undirected ties, the sociality parameters (the a_i s) would disappear, leaving $s(\cdot, \cdot)$ as a monotonic function of the natural distance metric, ϕ , on the unit hypersphere. However, although $s(\cdot, \cdot)$ is not a distance metric itself (since, for example, it is not nonnegative), it is a popular similarity measure: cosine similarity. Compared to a true latent distance model on the unit hypersphere, this choice of $s(\cdot, \cdot)$ changes the interpretation of α (and β) in model 2.1 and also re-weights the distances, since $\cos\phi$ is a non-linear function of ϕ .

McCormick and Zheng (2015) extend this model to the setting of aggregated

relational data (ARD), an example of incomplete network data. In this setting, surveyed individuals answer “how many X ’s do you know?,” where X represents particular, typically hard-to-reach, groups of interest such as drug users, terrorists, or homeless individuals. Thus, rather than observe the entire network, we only observe connections between surveyed individuals and the groups of interest; we do not observe ties between surveyed individuals and actual members of the group nor ties between members of the group. To accommodate this type of data, the authors first propose a model for the complete case (if the network had been entirely observed) and then derive a model for the aggregated observations. The proposed model for the complete case is a slight extension of [Hoff, Raftery and Handcock \(2002\)](#)’s projection model, where cosine similarity is again incorporated:

$$s(z_i, z_j) = a_i + a_j + \zeta z_i' z_j,$$

where a_i is a gregariousness or sociality effect for the i th node and ζ scales the overall influence of the latent component. Compared to [Hoff, Raftery and Handcock \(2002\)](#)’s projection model, [McCormick and Zheng \(2015\)](#) specify a sociality effect that is additive rather than multiplicative and that accounts for differences between the sender and the receiver. They also incorporate an additional scale parameter, ζ , which modifies the influence of the latent vectors. Latent positions for the survey participants are modeled as uniformly distributed across the hypersphere.

3.1.3 Other Spaces Although both the SBM and MMSBM allow for geometric interpretations of the latent vectors (i.e., as positions on the simplex), neither is an example of a latent distance model². Although some metrics have been developed in the context of compositional data, they generally are only intended for points on the open simplex and exclude points on the boundary. For example, of the popular Aitchison distance metric defined for the open simplex, [Aitchison et al. \(2000\)](#) note that when one of the coordinates of a point in the simplex tends to zero, the distance between it and other points in the simplex will tend toward infinity. The authors explain, “There is nothing surprising about this feature; it is merely recognizing that a composition with one of the parts absent may be chemically, physically, or biologically completely different from compositions with all components positive. Doveton’s (1998) perfect martini with its (gin, dry martini, sweet martini) composition is completely different from a cocktail with no gin but only dry and sweet martini present.” For compositional data, this may be a natural assumption but it is not clear whether it is necessary in the setting of latent membership vectors.

In [Schweinberger and Snijders \(2003\)](#), the authors specify a latent distance model in an ultrametric latent space. Unlike other versions of the latent space models considered here, this model does not specify \mathcal{Z}^t as a traditional metric space. Recall that a metric space consists of a set, M , and distance (metric), d , which satisfies the following properties for all points x, y , and $z \in M$:

²Of course, utilizing $s(z_i, z_j) = -d(z_i, z_j)$ in the original stochastic block model is meaningless, since all vertices of the simplex are, by design, equidistant. In the mixed-membership stochastic block model, this choice would significantly change the interpretation of the model: from a node’s tie probabilities depending on a weighted sum of the between-class tie probabilities, weighted by the node’s membership vector, to a node’s tie probabilities depending on distances in the space of all membership vectors.

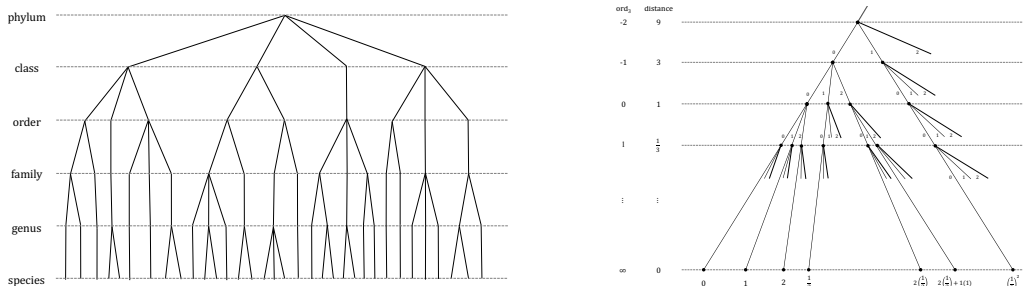


FIG 3. Examples of Ultrametric Space

1. Non-Negativity: $d(x, y) \geq 0$.
2. Identity of Indiscernibles: $d(x, y) = 0 \iff x = y$.
3. Symmetry: $d(x, y) = d(y, x)$.
4. Triangle Inequality: $d(x, z) \leq d(x, y) + d(y, z)$.

An ultrametric space, or non-Archimedean space, is a metric space where d additionally satisfies the strong triangle inequality:

$$d(x, z) \leq \max \{d(x, y), d(y, z)\},$$

which, among other things, means that all triangles are isosceles with the unequal side being shortest and that every point in a disc is a center of that disc, so that two discs intersect only if one disc completely contains the other. Not surprisingly, visualizing an ultrametric space and understanding the behavior of distances within it can be difficult. However, ultrametric space can be visualized via dendograms or trees. For example, \mathbb{Q}_p , the field of p -adic numbers, is a well-known ultrametric space which can be visualized as the tree in the right panel of Figure 3 (see [Holly, 2001](#), for a thorough motivation of this figure). For simplicity, consider a tree of the familiar animal species classification system in the right panel of Figure 3. Naturally, the distance between species is the height of the smallest (inverted) tree between them so that, for example, species within the same genus are closer ($d=1$) than those who only share a common order ($d=3$).

Schweinberger and Snijders (2003) motivate this choice for \mathcal{Z}^t by noting that social scientists' understanding of latent settings³ structures mimic properties guaranteed in ultrametric spaces. More specifically, the latent settings should be non-overlapping, the interaction within settings should be stronger than the interaction between settings, and hierarchical nesting of the settings is expected. The authors fit the model to a fraternity interaction network and provide a topological map (e.g. Figure 4) of the estimated latent positions where each level of the mapped social “mountain” can be interpreted as a social setting. An example of the style of resulting settings groups is provided in Figure 4

3.2 Hyperbolic Space

Recent work in latent space models for network data has resulted in a novel proposal: the use of negatively curved t -dimensional hyperbolic space, \mathbb{H}^t . First suggested by [Krioukov et al. \(2010\)](#), modeling and analyzing networks in latent

³Here, the authors refer to the settings terminology emphasized by Pattison and Robins (2002) where a setting is a close-knit cluster of actors that are strongly tied.

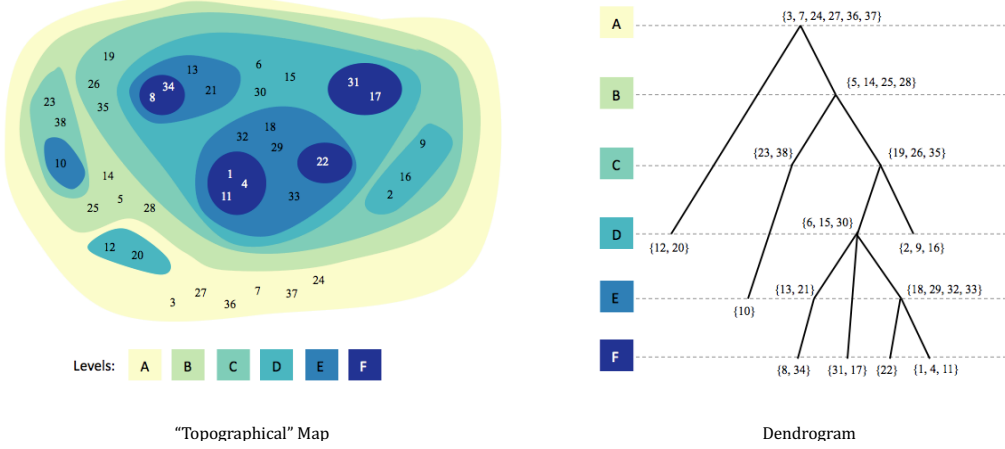


FIG 4. *Positions in a Latent Ultrametric Space.* As a toy example, we plot “positions” in a latent ultrametric space, visualized above in the style of a topographical map, on the left, and as a dendrogram, on the right. Colors represent the levels and the nodes are indexed arbitrarily. Note that nodes’ relative positions within a particular level in the topographical map are meaningless and are simply an artifact of this particular visualization.

hyperbolic spaces is rapidly being investigated (Aldecoa, Orsini and Krioukov, 2015; Asta and Shalizi, 2014; Smith, 2017, among others). A generic latent distance model in 2-dimensional hyperbolic space can be written as follows:

$$\begin{aligned}
 (3.1) \quad & Y_{ij} \stackrel{ind}{\sim} \text{Bernoulli}(p_{ij}) \\
 & \text{logit}(p_{ij}) = \alpha - d(z_i, z_j) \\
 & z_i \in \mathbb{H}^2, \quad z_i \stackrel{ind}{\sim} f_2(z|\psi)
 \end{aligned}$$

where

$$\begin{aligned}
 (3.2) \quad & d(z_i, z_j) = d((r_i, \phi_i), (r_j, \phi_j)) \\
 & = \text{acosh} \{ \cosh(r_i) \cosh(r_j) - \sinh(r_i) \sinh(r_j) \cos(\Delta\phi) \}
 \end{aligned}$$

and

$$\Delta\phi = \pi - |\pi - |\phi_i - \phi_j||,$$

so that $d(z_i, z_j)$ is the appropriate distance metric in hyperbolic space (using polar coordinates for convenience) and $f_2(z|\psi)$ is a distribution for positions in 2-dimensional hyperbolic latent space (extending this specification to t -dimensional hyperbolic space is trivial). Of course, the exact form of this model and the choice of $f_t(z|\psi)$ can be altered - perhaps to respect particular network features or to accommodate different network modeling assumptions.

Krioukov et al. (2010) provides a thorough motivation for the use of hyperbolic space in the class of latent space models for network data, stemming from the observation that many real world networks tend to be tree-like and that the geometry of a tree behaves much like the geometry of hyperbolic space. Informally, trees can be thought of as discrete hyperbolic spaces since \mathbb{H}^2 can be constructed as metrically equivalent to b -ary trees, trees with a branching factor of b . Further,

the number of nodes at distance (path length) r in a b -ary tree grows exponentially. Thus, trees need an exponential amount of space for branching and only hyperbolic space is able to accommodate this since hyperbolic space is “bigger” than Euclidean space. For example, consider linearly increasing the radius of a sphere; in Euclidean space, the circumference of the sphere also grows linearly, but in hyperbolic space the circumference grows exponentially.

The fact that hyperbolic space has “more space” than Euclidean space has also been used to help visualize large networks (Lamping, Rao and Pirolli, 1995; Munzner, 1997). For example, visualizing a network in the Poincaré disk (see Appendix A and Figure 10 for a more detailed description of the Poincaré disk) is like viewing the network through a fish-eye lens, with nodes at the center of the disk in focus and displayed with the most detail while nodes that are further away are pushed towards the boundary of the disk and are diminished in size. In fact, because hyperbolic space is “bigger” than Euclidean space, it cannot be exactly embedded within it. Thus, unlike elliptic space where we can, for example, easily picture the surface of a hypersphere in \mathbb{R}^3 , there exist many models for visualizing hyperbolic space, each of which highlights different features of hyperbolic geometry (see Appendix A for more details).

Krioukov et al. (2010) also provide a higher-level argument based on the observed hierarchical structure of many real world networks (Clauset, Moore and Newman, 2008). More specifically, note that networks, by definition, connect heterogeneous nodes. Consider the familiar example of a social network, where the nodes represent individuals who may have different genders, ages, family backgrounds, etc. This heterogeneity implies that some sort of classification or grouping exists. We can imagine grouping the nodes of a social network first by gender, then by age group within gender, etc., creating a hidden hierarchical structure. Finally, the relationships among these groups could be represented as a tree-like structure. Thus, networks can be thought of as (even approximate) trees, which we have already described as living in hyperbolic space. And in fact, many networks exhibit tree-like characteristics (see, for example, Abu-Ata and Dragan, 2016). Note that this line of thought mirrors the justification for the use of ultrametric space provided by Schweinberger and Snijders (2003). In fact, ultrametric spaces are very closely related to hyperbolic space (see, for example Ibragimov, 2014). However, in generic hyperbolic space, the natural distance metric does not satisfy the strong triangle inequality.

The key aspect of hyperbolic space which allows for a tree’s exponential branching and which can accommodate complex network structure is its negative curvature. This directly influences the behavior of familiar geometric properties in hyperbolic space. For example, triangles in hyperbolic space appear skinny or thin, with the sum of their angles being less than 180° (see Table 1). Similarly, distances in hyperbolic space behave differently than those in Euclidean space. For example, in Figure 5 we simulate 500 points in 2-dimensional hyperbolic space (using the hyperboloid model of \mathbb{H}^2 for visualization and simulating points uniformly⁴ within a disk of radius R), and connect all points within $\gamma = R$ units of each other. This is equivalent to replacing the logit link function in model 3.1 with a Heaviside step function, $p_{ij} = \Theta\{\gamma - d(z_i, z_j)\}$, where the Heaviside step

⁴See equation 3.3 and the following discussion for a more detailed description of the uniform distribution for discs in hyperbolic space.

TABLE 1
Geometric Properties of Curved Spaces. This table is adapted from Krioukov et al. (2010).

	GEOMETRY		
	Euclidean	Spherical	Hyperbolic
Curvature, K	0	> 0	< 0
Number of parallel lines	1	0	∞
PROPERTY			
Triangles look...	normal	thick	thin
Sum of angles in a triangle	π	$> \pi$	$< \pi$
Circumference of a circle	$2\pi r$	$2\pi \sin(\sqrt{ K }r)$	$2\pi \sinh(\sqrt{ K }r)$
...as r increases,	linear growth	-	exponential growth

function is defined by

$$\Theta(x) = \begin{cases} 1 & x \geq 0 \\ 0 & \text{otherwise.} \end{cases}$$

Of course, rather than deterministically connecting points within a certain distance, we could easily utilize the original model outlined in 3.1. However, although the probabilistic link function allows for greater variation in simulated networks, the Heaviside step function instead emphasizes the role of the distance metric in the latent space network model. In the left panel of Figure 5, we have also drawn circles of radius $\gamma = R$ about two particular simulated points. First, it should be clear that distances behave differently in hyperbolic space, since these circles look very different than what we would expect in Euclidean space. Second, note that most of the lines or connections are radially oriented. In fact, if we imagine this simple simulation as a toy latent space network model, we see that this tendency towards radially oriented connections might create networks that have heterogeneous degree distributions and are more centralized. Points or nodes near the base of the hyperbola are the more central nodes in the network, with lots of connections to nodes further from the origin, near the periphery. These peripheral nodes have fewer connections to the less central nodes along the periphery (fewer connections to other nodes that are also far from the origin) and are most likely connected to the central nodes near the origin. This type of centralization is often observed in real world networks and, for the latent space model, is simply an artifact of the negative curvature of the latent hyperbolic space.

Similarly, we can mimic this construction in positively-curved space, embedding nodes on the surface of a 3-dimensional hypersphere as suggested by Hoff, Raftery and Handcock (2002) and McCormick and Zheng (2015). In the right panel of Figure 5 we simulate 500 points on the surface of the upper half of a 2-

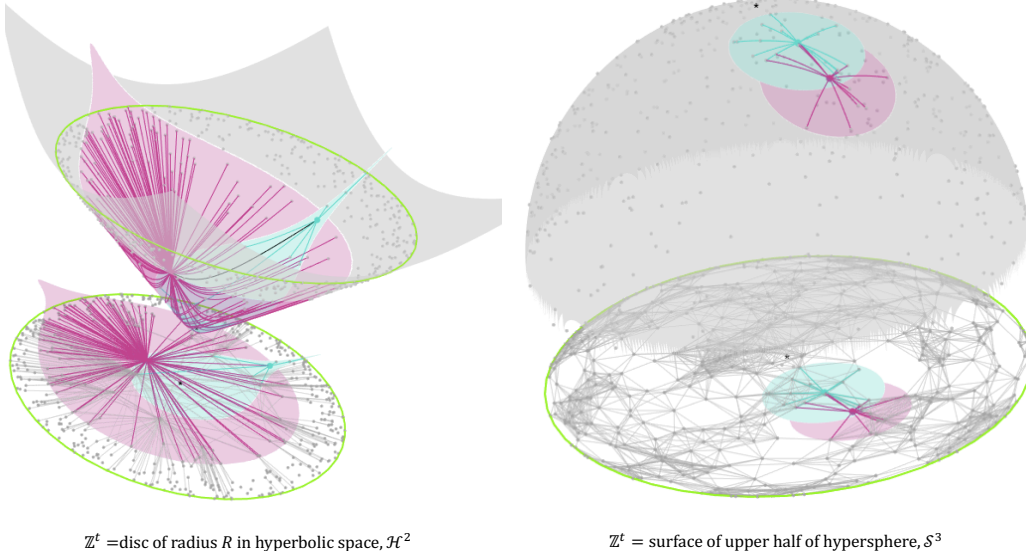


FIG 5. *Networks Simulated in Complex Geometries* ($n = 500$ nodes). In each panel, we highlight two nodes by drawing circles of radius R about them and color their connections to other nodes in the network.

dimensional hypersphere (naturally visualized in 3-dimensional Euclidean space), again simulating points uniformly across this space. Again, we use the toy version of the latent distance model which incorporates the Heaviside step function, so that all points within $\gamma = R$ units of each other are connected. Note that the hyperbolic space's striking pattern of radially oriented ties does not appear in positively-curved space, indicating that we will not see much centralization or heterogeneity of the degree distribution. Instead, the network simulated on the surface of the hypersphere appears to have more community structure, with sets of nodes that are highly interconnected but have fewer connections to other nodes outside of their set. To our knowledge, there has been no formal development of theoretical or practical reasons as to why positively-curved space might be particularly amenable to latent space models for network data. However, in [McCormick and Zheng \(2015\)](#)'s application of this model to aggregated relational data, the authors mention a few appealing characteristics of working on the surface of a hypersphere. First, calculations are simplified by the fact that the space is finite so that there is no need to restrict latent positions to some subset of the space (i.e., a (finite) disk of radius R in (infinite) hyperbolic space). Second, because the space is finite, this provides a natural non-zero lower bound for the probability of a tie in the network. This assumption is more amenable to many practical settings, especially for aggregated relational data since the probability that an individual is tied to at least one member of a relatively large group of individuals is likely nonzero in practice.

[Krioukov et al. \(2010\)](#) derive a hyperbolic latent space model which directly connects model parameters to important features of network structure, but departs from our specification of a generic latent space model in [2.1](#). The authors

outline the following model in \mathbb{H}^2 :

$$(3.3) \quad \begin{aligned} Y_{ij} &\stackrel{ind}{\sim} \text{Bernoulli}(p_{ij}) \\ \text{logit}(p_{ij}) &= \frac{1}{2T} \{ R(n, \bar{k}, \gamma, T) - d(\mathbf{z}_i, \mathbf{z}_j) \} \\ r_i &\stackrel{iid}{\sim} p(r|R, \alpha(\gamma, T)), \quad \phi_i \stackrel{iid}{\sim} \text{Uniform}(0, 2\pi), \end{aligned}$$

where the latent positions are specified in polar coordinates, $\mathbf{z}_i = (r_i, \phi_i)$ and distance between the i th and j th latent position is given by 3.2. The latent positions are assumed to be quasi-uniformly distributed within a disk of radius R centered at the origin,

$$p(r|R, \alpha) = \alpha \frac{\sinh(\alpha r)}{\cosh(\alpha R) - 1}, \quad \alpha = \begin{cases} \frac{1}{2}(\gamma - 1), & T \leq 1 \\ \frac{1}{2T}(\gamma - 1), & T > 1, \end{cases}$$

which is roughly equivalent to an $\text{Exponential}(\alpha)$ distribution. Note that $p(r|R, \alpha)$ distributes points exactly uniformly within a disk of radius R when $\alpha = 1$. In the model, the radius of this disk is a function of expected network characteristics, $R \equiv R(n, \bar{k}, \gamma, T)$ where \bar{k} is the expected average degree, γ is the exponent of the power-law degree distribution, and T controls the amount of clustering, and satisfies the following equation:

$$\bar{k} = \frac{N}{\pi} \int_0^R p(r_1|R, \alpha) \int_0^R p(r_2|R, \alpha) \int_0^\pi \text{logit}(p_{ij}) d\phi_1 dr_1 dr_2.$$

In practice, numerical integration is used to calculate R which complicates potential inference for this particular specification of the model.

4. IMPLICATIONS OF LATENT SPACE GEOMETRY ON NETWORK SUMMARY STATISTICS

Of course, Krioukov et al. (2010)'s line of reasoning - that the negative curvature of hyperbolic geometry accommodates complex network structure - leads to a rather natural question: what role does the curvature of the latent space play in latent space models for network data? By considering networks simulated from latent distance models in spaces of varying curvature, we will explore the function of geometric curvature in the latent space model. Further, we show that, for the purposes of building a hierarchical network model, changing the geometry of the latent space can parsimoniously grow the complexity of the latent space network model while maintaining the intuitive appeal of using distance to model dependence.

For consistency, we will hold the distribution of latent positions constant across all spaces. Here, we have chosen to assume that the latent positions are uniformly distributed within a disk of radius R , where R is specified such that all three latent spaces have the same diameter (maximum distance between pairs of points)⁵. Although we might consider directly examining simulated networks under each of these models, binary data can be particularly difficult to study and binary relational data (i.e., networks) are no exception. For example, in the latent

⁵For hyperbolic latent space, we choose R according to the approximation provided by Krioukov et al. (2010, equation 13), corresponding to an average degree of eight.

space model, even if p_{ij} smoothly varies across potential ties in the network, this smoothness can not be manifested in the observed network, since observed ties are by definition either present or absent. Thus, in our simulation study, we use a Heaviside step link function as was utilized in Figure 5, again to emphasize the roles of the different distance metrics in each latent geometry. Here, we consider smoothly varying γ , the Heaviside step function cut point, and examining differences in network structure across three latent geometries: Euclidean space, hyperbolic space, and elliptic space. The model used in this simulation exercise, is thus as follows:

$$(4.1) \quad \begin{aligned} Y_{ij} &= \Theta\{\gamma - d(z_i, z_j)\} & i < j; \quad i, j = 1, \dots, n \\ z_i &\in \mathcal{Z}^t, \quad z_i \stackrel{iid}{\sim} \text{Uniform}(R) \quad i = 1, \dots, n, \end{aligned}$$

which is equivalent to replacing the logit link function in model 3.1 with the Heaviside step function. In this case, the tie variables, Y_{ij} , can still technically be written as Bernoulli variables but are actually deterministically, rather than probabilistically, specified. Of course, while these choices greatly simplify the model originally outlined by 3.1, they allow us to more directly consider the role of geometry in the latent space model for network data.

First, it is worth noting that the typical distribution of distances varies greatly across these geometries. For example, consider distances from a set of points simulated under each model⁶ in Figure 6. In Euclidean space, the distribution of distances is skewed right, with most points close together and only a few points very far apart. The distribution of distances for latent positions on the hyperboloid looks very different than for those in Euclidean space. In hyperbolic space, there are few points that are very close together and the distribution of distances is left skewed. This distribution likely better represents our intuition about the distances between latent positions for nodes in real world social networks - any randomly selected pair of individuals is not likely to have a tie (i.e., any pair of positions is likely far apart). In Elliptic space, the distribution of distances is much more symmetric. Recall that we have chosen the same distribution for the latent positions (uniform within a disk of radius R) across all three geometries, so that observed differences in the distributions of the distances in Figure 6 is due to the differing curvature of the spaces.

Naturally, one can imagine how these differences in the distribution of distances might affect a network's degree distribution. In the social network setting, a Euclidean latent space implies that most individuals are very social, but there may be a few loners (a few actors with very few ties); a hyperbolic space implies that most individuals are asocial with only a few very popular actors; and an elliptic space implies that there are some loners and some popular actors, but most actors display the same level of sociality. Of course, our description of the intuitive degree distribution in a hyperbolic latent space is a natural way of describing degree heterogeneity, a long observed trait of many real world networks.

The results of our simulation study where we vary the cut point in the Heaviside step function, γ , and examine changes in network features is displayed in Figures 7 and 8. Naturally, the range of the distances varies across the latent geometries (consider the x -axes of the histograms in Figure 6). In our simulation

⁶Variation across simulations does not appear to impact the conclusions drawn here.

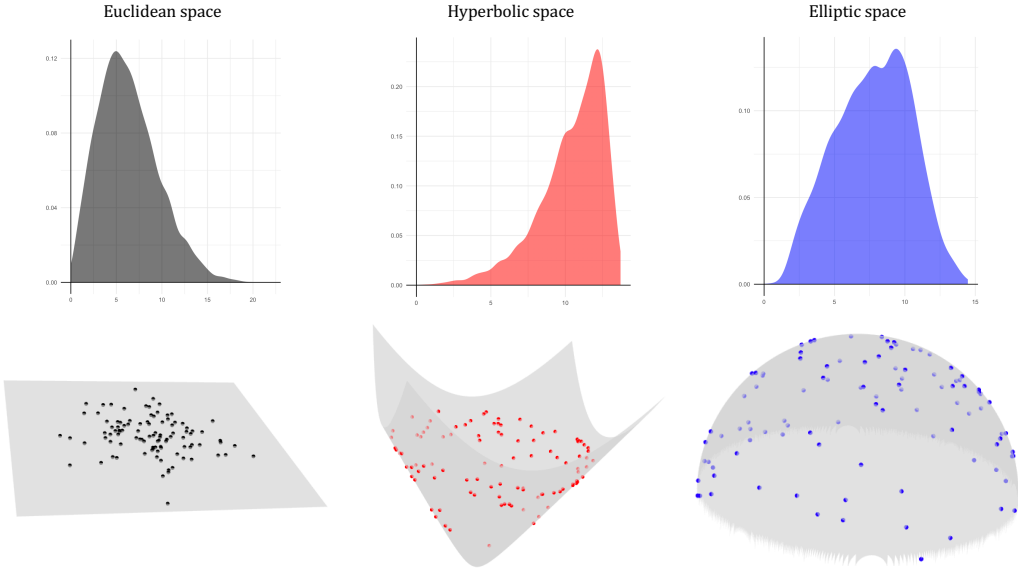


FIG 6. *Distribution of Distances in Latent Spaces with Differing Geometries.* Panels in the bottom row plot points simulated in Euclidean, hyperbolic, and elliptic space, respectively, while panels in the top row plot histograms of the pairwise distances for these sets of points.

exercise, we accommodate for this difference in scaling by dividing the distances by the maximum simulated distance in each simulation, so that all distances are contained within $[0, 1]$. We consider networks of various size ($n = 20, 50, 100$) embedded in Euclidean, hyperbolic, and elliptic latent geometries. For each geometry and network size considered, we simulate 100 networks according to model 4.1, and slowly increase γ from 0 to 1 by increments of 0.20. We plot the average of common network summary measures - clustering, average path length, degree centrality, betweenness centrality, closeness centrality, and modularity - of the resulting simulated networks as a function of γ in Figures 7 and 8. Bands on these plots are pointwise minima and maxima across the simulations - the jaggedness of these bands is a consequence of finite size effects for the simulated networks.

In Figure 7, we compare networks in hyperbolic space to those in Euclidean space. Note that networks in hyperbolic space can achieve much higher levels of degree centrality, closeness, and betweenness and that this effect is more prominent for larger networks. This coincides with our previous intuition for the behavior of the degree distribution of networks in hyperbolic space. Note also, that this improved ability to model degree heterogeneity does not come at the expense of any loss to clustering or average path length. In Figure 7, we see that networks in elliptic space do not differ greatly from those in Euclidean space. Although this may seem counterintuitive, reconsider the simulated network on the surface of the hypersphere in Figure 5. Recall that the only “obvious” feature of this network is some indication of a community structure, with distinct groups of nodes having more connections within the group and fewer connections across groups. And in fact, we see some difference in the modularity statistics across the two spaces.

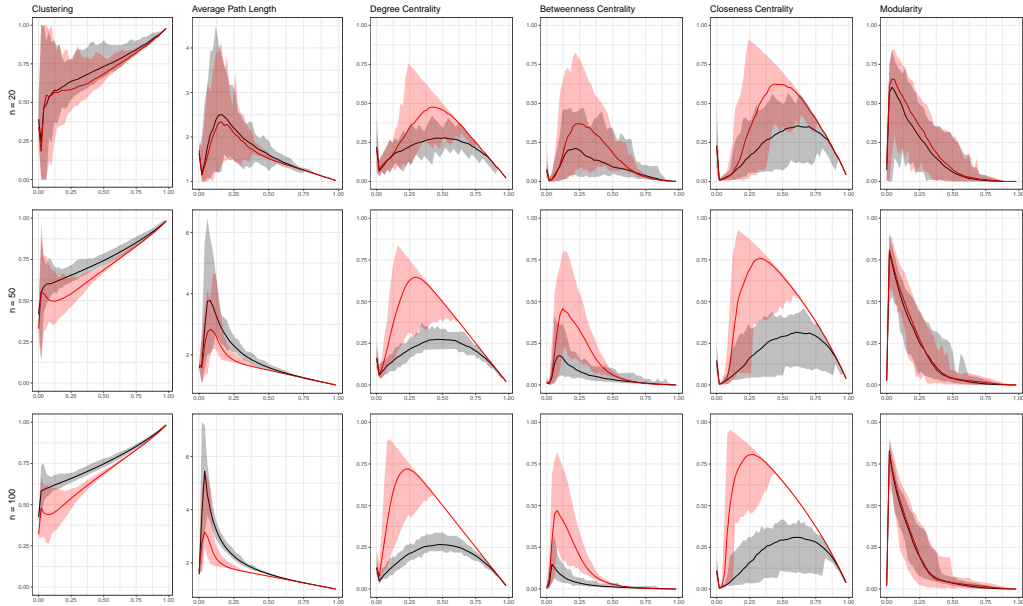


FIG 7. *Network Statistics in Hyperbolic Space.* The x -axis is γ , the Heaviside step function cut point. Distances across the geometries are made comparable by re-scaling each simulation to the $[0, 1]$ interval. Each row of plots corresponds to simulated networks of a different size, $n = 20, 50, 100$, and each column of plots corresponds to a different network summary measure. Red simulated network statistics are derived from networks with a hyperbolic latent space and black network statistics are derived from networks with a latent Euclidean space.

5. USING GRAPH LAPLACIANS TO IDENTIFY AN APPROPRIATE GEOMETRY

As mentioned above, many common descriptive summary measures of network structure are sensitive to the size of the network. Thus, while the behavior of these measures across latent spaces of different geometries can provide us with some indication of the role of geometry in these models, it can not provide a complete picture. This issue is rooted in the fact that it is difficult to find a common language describing both networks and geometric spaces; such a common language is a prerequisite for comparing properties between the two sorts of structures. However, as we will examine in this section, both the geometry of a space and the combinatorics of a graph or network can be described by linear operators whose eigenvalues are comparable.

For geometric spaces, the Laplace-Beltrami operator, ∇_M^2 , is an operator on smooth functions which map general Riemannian manifolds, M , to \mathbb{R} . For a function, $f = f(x_1, x_2, \dots, x_n)$, when $M = \mathbb{R}^n$, the Laplace-Beltrami operator can be expressed in terms of partial derivatives:

$$(5.1) \quad \nabla_{\mathbb{R}^n}^2 f = \sum_{i=1}^n \frac{\partial^2 f}{\partial x_i^2}.$$

and hence when $M = \mathbb{R}$, the Laplace-Beltrami operator is simply the second derivative, $\nabla_{\mathbb{R}}^2 f = f''$. Even for general Riemannian manifolds, M , the Laplace-Beltrami operator, ∇_M^2 , is essentially defined by 5.1 with respect to local coordinates x_1, x_2, \dots, x_n . The eigenvalues of the Laplace-Beltrami operator describe

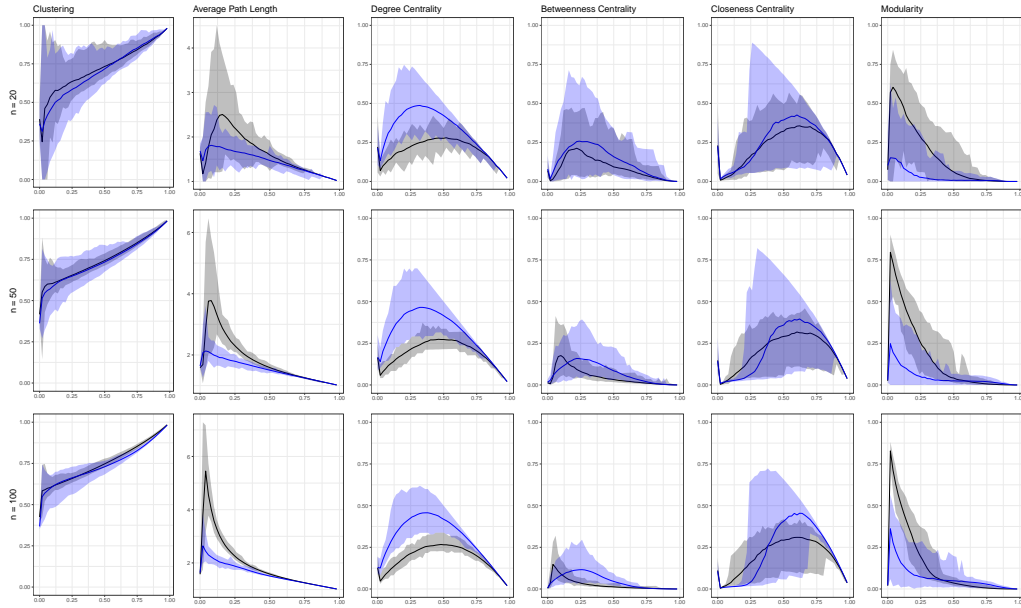


FIG 8. *Network Statistics in Elliptic Space.* The x -axis is γ , the Heaviside step function cut point. Distances across the geometries are made comparable by re-scaling each simulation to the $[0, 1]$ interval. Each row of plots corresponds to simulated networks of a different size, $n = 20, 50, 100$, and each column of plots corresponds to a different network summary measure. Blue simulated network statistics are derived from networks with a latent elliptic space (on the surface of a hypersphere) and black network statistics are derived from networks with a latent Euclidean space.

many (though not all) geometric properties of the space M . The first positive eigenvalue of the Laplace-Beltrami operator is positively related to the curvatures of certain compact manifolds (Lichnerowicz, 1958). More generally, a conjectural generalization of Weyl's Law (Weyl, 1911) describes a relationship between the volumes of compact domains D in any Riemannian manifold M and the eigenvalues of the Laplace-Beltrami operator ∇_M^2 , restricted to those functions with support D (Ivrii, 1980). Thus, in particular settings, we can describe a direct relationship between the eigenvalues of the Laplace-Beltrami operator and the geometry of a space.

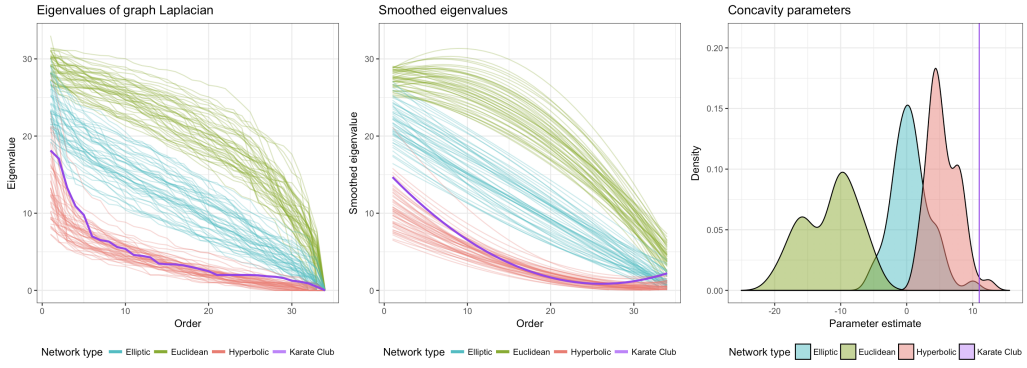
For network data, the *graph Laplacian*, ∇_G^2 , of a graph G is the operator on functions which map the set of vertices of the network, v_1, v_2, \dots, v_n , to \mathbb{R} and is defined by:

$$(\nabla_G^2)(v_i) = \left(\sum_{Y_{ij}=1} f(v_j) \right) - \deg(v_i).$$

We can understand this formula intuitively by considering its correspondence with the Laplace-Beltrami operator and the second derivative of a function in \mathbb{R}^n . Just as a discrete analogue of the derivative is a difference between successive values of f , $\nabla_G^2 f$ is the difference of such differences,

$$(\nabla_G^2 f)(v_i) = [f(v_{i-1}) - f(v_i)] - [f(v_i) - f(v_{i+1})]$$

for $1 < i < n$ whenever G is the discrete, graph-theoretic approximation of \mathbb{R} in

FIG 9. *Eigenvalues of Graph Laplacians.*

the sense that

$$v_1 \rightarrow v_2 \rightarrow \cdots \rightarrow v_n.$$

The eigenvalues of the graph Laplacian, ∇_G^2 , describe many (though not all) combinatorial features of the graph G . For example, the algebraic multiplicity of the eigenvalue 0 reveals how many connected components G has. The second smallest eigenvalue of ∇_G^2 quantifies how interconnected the nodes in G are.

For both geometric spaces and network data, the linear operators described above (the Laplace-Beltrami operator for geometric spaces and the graph Laplacian for network data) provide us with eigenvalues that describe natural features of these very different mathematical structures. Furthermore, these linear operators have been shown to be closely related, under certain conditions. Specifically, if we consider graphs formed by taking nodes as points in M and weighting edges between vertices according to distances in M , it can be shown that the Laplace-Beltrami operator is the limit, in one sense or the other, of the graph Laplacians (c.f. [Belkin and Niyogi, 2005](#); [Ting, Huang and Jordan, 2011](#); [Hein, Audibert and Luxburg, 2007](#)). Unfortunately, these results do not directly imply that the eigenvalues of the graph Laplacians for unweighted graphs generated by our CLS models in particular latent spaces will converge to the eigenvalues of the Laplace-Beltrami operator. Moreover, these results do not apply to non-manifolds, such as closed disks in Euclidean and hyperbolic spaces. Some recent work ([Belkin et al., 2012](#)) indicates that the graph Laplacians are dramatically affected by the presence of boundaries, such as the boundary circles of closed disks. Nonetheless, we intuitively expect the eigenvalues of the graph Laplacians for network data generated from CLS models to be able to help identify the latent spaces that helped generate them.

We test this intuition with some simulations. As in Section 4, we consider models where nodes are uniformly distributed within a disk of radius R in Euclidean, hyperbolic, and elliptic latent space. As before, R is chosen such that all three spaces have the same diameter (maximum distance between pairs of points). In this setting, we generate 50 simulated networks, each with 34 nodes, for each CLS model. We also examine a standard social network studied in the literature having 34 nodes, Zachary's Karate Club network ([Zachary, 1977](#)). In the far left panel of Figure 9, plots of the eigenvalues in decreasing order strongly suggest that Zachary's Karate Club network exhibits geometric features strongly

reminiscent of hyperbolic space.

Furthermore, Weyl's Law and its generalizations strongly suggest (although do not directly imply) that the rate at which the eigenvalues increase should strongly correlate with the rate at which areas of disks grow as a function of radius. Thus motivated, in the far right panel of Figure 9, we also fit a quadratic curve to each of the network's series of eigenvalues (these curves are displayed in the center panel of Figure 9) and compare the concavities, i.e. the second derivatives of the fitted curves. The distribution of these concavity parameters across the different latent space geometries more clearly delineates the role of geometry in network structure.

6. DISCUSSION

As we have demonstrated in this simulation exercise, using a negatively curved latent space allows us to smoothly grow the complexity of the latent space model (i.e., accommodate more complicated network structure, as was expected from the intuitive arguments provided by [Krioukov et al., 2010](#), and as was demonstrated in Figure 7) without adding any additional structure to the model, such as explicit functions of network statistics as is done in ERGMs, or node-level random effects such as ([Hoff, 2005](#); [Krivitsky et al., 2009](#)), or mixture distributions to spatially cluster the latent positions as in ([Handcock, Raftery and Tantrum, 2007](#)). Furthermore, this version of the model preserves the use of distance to model dependence, a common feature of many popular statistical models, and is able to draw upon the long success of latent space models for network data. We have provided evidence that the switch from Euclidean to hyperbolic latent spaces makes the generated networks align more closely to real-world networks in local and global structure (e.g. Figure 9).

Of course, many open questions about the relationship between geometric curvature and network properties remain unanswered. For example, what is the precise role of the distribution for the latent positions in a geometric space of a particular curvature? Future work might also consider continuing this investigation by considering a parametric family of spaces parametrized by their curvature, δ : from spaces of negative curvature ($\delta < 0$) to Euclidean space ($\delta = 0$) to spaces with positive curvature ($\delta > 0$). In this setting, we might imagine modeling observed networks by averaging over features of networks from both hyperbolic and elliptic space, for example. We might also imagine performing inference for δ and using estimates of δ to describe properties of the observed network, or perhaps, to make comparisons across a set of observed networks.

Another exciting line of future research might consider a flipped perspective on the discussion provided here. More specifically, given a particular set of network data can we use summary measures of observed network structure and/or graph Laplacians to infer the appropriate latent space geometry. This type of approach might prove useful in model selection.

APPENDIX A: MODELS FOR VISUALIZING HYPERBOLIC SPACE

First, note that hyperbolic space is an example of a non-Euclidean space. Recall that Euclidean space is described by Euclid's five postulates:

1. Each pair of points can be joined by one and only one straight line segment.

2. Any straight line segment can be indefinitely extended in either direction.
3. There is exactly one circle of any given radius with any given center.
4. All right angles are congruent to one another.
5. Given any straight line and a point not on it, there exists one and only one straight line which passes through that point and never intersects the first line, no matter how far they are extended.

where the last postulate is referred to as the “parallel postulate.” Non-Euclidean spaces are formed by replacing the parallel postulate with some alternate behavior. In hyperbolic space, it is replaced with the following:

- 5*. Given any straight line and a point not on it, there are at least two distinct lines passing through that point which do not intersect with the line.

Thus, in hyperbolic space, there exists infinitely many parallel lines. In order to visualize the geometric properties of hyperbolic space, there are four popular analytic models: the Beltrami-Klein model, the Poincaré disk model, the Poincaré half-plane model, and the hyperboloid model (although other models certainly exist). Each of these models define a hyperbolic plane which satisfies the axioms of a hyperbolic geometry (1,2,3,4, and 5*). Moving forward, we will primarily rely on the hyperboloid model to visualize positions in hyperbolic space but will sometimes refer to the Poincaré disk model as well.

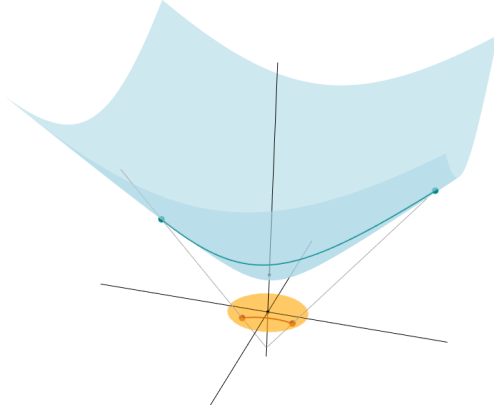


FIG 10. *Visualizing Hyperbolic Space.* Turquoise points are plotted on the hyperboloid model (light blue), where the shortest distance between two points is a line across the surface of the hyperboloid. Orange points are plotted on the Poincaré model, where the shortest distance between two points is the arc of the circle which intersects the two points and is perpendicular to the boundary. Points in the Poincaré model are stereographic projections of points in the hyperboloid model - imagine sitting at $z = -1$ and looking through a disk of radius one, centered at $z = 0$, up at the points on the hyperboloid (grey lines).

Hyperboloid model. Although specified for n -dimensional hyperbolic space, we will typically focus on a 2-dimensional hyperbolic space, \mathbb{H}^2 , and describe this version of the model here. Points on the hyperbolic plane are modeled as points on the surface of the upper (or lower) sheet of a hyperboloid in 3-dimensional Euclidean space, \mathbb{R}^3 (consider the blue points in Figure 10). That is, all points

(x, y, z) in the plane satisfy the following

$$z^2 - y^2 - x^2 = 1,$$

with $z > 0$. Distance between points in the hyperboloid model is simply distance along the surface of the hyperboloid; this mimics visualization of distance in elliptic space, as the distance (arc length) along the surface of the hypersphere.

Poincaré disk model. Unlike the hyperboloid model, the Poincaré disk model represents (infinite) hyperbolic space within a finite space. This model is formed by the stereographic projection of the hyperboloid in \mathbb{R}^3 onto the unit disc at $z = 0$. As points in this model move closer to the boundary of the disk, they approach infinity; in the hyperboloid model, this is equivalent to moving further up the surface of the hyperboloid (consider the orange points in Figure 10). Distances in this model are semicircles perpendicular to the boundary of the Poincaré disk.

ACKNOWLEDGEMENTS

Smith and Calder were partially supported by grants from the National Science Foundation (NSF DMS-1209161), the National Institutes of Health (NIH R01 HD088545), and The Ohio State University Institute for Population Research (NIH P2CHD058484).

REFERENCES

ABU-ATA, M. and DRAGAN, F. F. (2016). Metric tree-like structures in real-world networks: an empirical study. *Networks* **67** 49–68.

AIROLDI, E. M., COSTA, T. B. and CHAN, S. H. (2013). Stochastic blockmodel approximation of a graphon: Theory and consistent estimation. In *Advances in Neural Information Processing Systems* 692–700.

AIROLDI, E. M., BLEI, D. M., FIENBERG, S. E. and XING, E. P. (2008). Mixed membership stochastic blockmodels. *Journal of Machine Learning Research* **9** 1981–2014.

AITCHISON, J., BARCELÓ-VIDAL, C., MARTÍN-FERNÁNDEZ, J. and PAWLOWSKY-GLAHN, V. (2000). Logratio analysis and compositional distance. *Mathematical Geology* **32** 271–275.

ALDECORA, R., ORSINI, C. and KRIOUKOV, D. (2015). Hyperbolic graph generator. *Computer Physics Communications* **196** 492–496.

ASTA, D. and SHALIZI, C. R. (2014). Geometric network comparison. under review, arXiv preprint 1411.1350.

BELKIN, M. and NIYOGI, P. (2005). Towards a theoretical foundation for Laplacian-based manifold methods. In *COLT* **3559** 486–500. Springer.

BELKIN, M., QUE, Q., WANG, Y. and ZHOU, X. (2012). Toward understanding complex spaces: Graph laplacians on manifolds with singularities and boundaries. In *Conference on Learning Theory* 36–1.

CHEH, K. and LEI, J. (2016). Network cross-validation for determining the number of communities in network data. *Journal of the American Statistical Association*.

CLAUSSET, A., MOORE, C. and NEWMAN, M. E. (2008). Hierarchical structure and the prediction of missing links in networks. *Nature*.

DIACONIS, P. and JANSON, S. (2007). Graph limits and exchangeable random graphs. *arXiv preprint arXiv:0712.2749*.

FRANK, O. and STRAUSS, D. (1986). Markov graphs. *Journal of the American Statistical Association* **81** 832–842.

HANDCOCK, M. S., RAFTERY, A. E. and TANTRUM, J. M. (2007). Model-based clustering for social networks. *Journal of the Royal Statistical Society: Series A (Statistics in Society)* **170** 301–354.

HEIN, M., AUDIBERT, J.-Y. and LUXBURG, U. v. (2007). Graph Laplacians and their convergence on random neighborhood graphs. *Journal of Machine Learning Research* **8** 1325–1368.

HOFF, P. D. (2005). Bilinear mixed-effects models for dyadic data. *Journal of the american Statistical association* **100** 286–295.

HOFF, P. (2008). Modeling homophily and stochastic equivalence in symmetric relational data. In *Advances in Neural Information Processing Systems* 657–664.

HOFF, P. D. (2009). Multiplicative latent factor models for description and prediction of social networks. *Computational and mathematical organization theory* **15** 261–272.

HOFF, P. D., RAFTERY, A. E. and HANDCOCK, M. S. (2002). Latent space approaches to social network analysis. *Journal of the american Statistical association* **97** 1090–1098.

HOLLAND, P. W. and LEINHARDT, S. (1970). A method for detecting structure in sociometric data. *American Journal of Sociology* 492–513.

HOLLY, J. E. (2001). Pictures of ultrametric spaces, the p-adic numbers, and valued fields. *The American Mathematical Monthly* **108** 721–728.

IBRAGIMOV, Z. (2014). A hyperbolic filling for ultrametric spaces. *Computational Methods and Function Theory* **14** 315–329.

IVRII, V. Y. (1980). Second term of the spectral asymptotic expansion of the Laplace-Beltrami operator on manifolds with boundary. *Functional Analysis and Its Applications* **14** 98–106.

KRIOUKOV, D., PAPADOPOULOS, F., KITSAK, M., VAHDAT, A. and BOGUNÁ, M. (2010). Hyperbolic geometry of complex networks. *Physical Review E* **82** 036106.

KRIVITSKY, P. N., HANDCOCK, M. S., RAFTERY, A. E. and HOFF, P. D. (2009). Representing degree distributions, clustering, and homophily in social networks with latent cluster random effects models. *Social networks* **31** 204–213.

LAMPING, J., RAO, R. and PIROLI, P. (1995). A focus+ context technique based on hyperbolic geometry for visualizing large hierarchies. In *Proceedings of the SIGCHI conference on Human factors in computing systems* 401–408. ACM Press/Addison-Wesley Publishing Co.

LAZARSFELD, P. F., HENRY, N. W. and ANDERSON, T. W. (1968). *Latent structure analysis* **109**. Houghton Mifflin Boston.

LICHNEROWICZ, A. (1958). Geometrie des groupes de transformations, Dunod, Paris, 1958. *Zentralblatt MATH* **96**.

LOVÁSZ, L. (2012). *Large networks and graph limits* **60**. American Mathematical Society Providence.

MCCORMICK, T. H. and ZHENG, T. (2015). Latent surface models for networks using aggregated relational data. *Journal of the American Statistical Association* **110** 1684–1695.

McMILLAN, A. and SMITH, A. (2016). When is nontrivial estimation possible for graphons and stochastic block models? *arXiv preprint arXiv:1604.01871*.

MINHAS, S., HOFF, P. D. and WARD, M. D. (2016). Inferential approaches for network analyses: AMEN for latent factor models. *arXiv preprint arXiv:1611.00460*.

MUNZNER, T. (1997). H3: Laying out large directed graphs in 3D hyperbolic space. In *Information Visualization, 1997. Proceedings., IEEE Symposium on* 2–10. IEEE.

NICKEL, C. L. M. (2007). Random dot product graphs: A model for social networks.

PAO, H., COPPERSMITH, G. A. and PRIEBE, C. E. (2011). Statistical inference on random graphs: Comparative power analyses via Monte Carlo. *Journal of Computational and Graphical Statistics* **20** 395–416.

PATTISON, P. and ROBINS, G. (2002). Neighborhood-based models for social networks. *Sociological Methodology* **32** 301–337.

SALDANA, D. F., YU, Y. and FENG, Y. (2015). How many communities are there? *Journal of Computational and Graphical Statistics*.

SCHWEINBERGER, M. and SNIJDERS, T. A. (2003). Settings in social networks: A measurement model. *Sociological Methodology* **33** 307–341.

SEWELL, D. K. and CHEN, Y. (2015). Latent space models for dynamic networks. *Journal of the American Statistical Association* **110** 1646–1657.

SMITH, A. L. (2017). Statistical methodology for multiple networks, PhD thesis, The Ohio State University.

SNIJDERS, T. A. and NOWICKI, K. (1997). Estimation and prediction for stochastic blockmodels for graphs with latent block structure. *Journal of classification* **14** 75–100.

SNIJDERS, T. A., PATTISON, P. E., ROBINS, G. L. and HANDCOCK, M. S. (2006). New specifications for exponential random graph models. *Sociological Methodology* **36** 99–153.

TING, D., HUANG, L. and JORDAN, M. (2011). An analysis of the convergence of graph Laplacians. *arXiv preprint arXiv:1101.5435*.

WEYL, H. (1911). Sur la distribution asymptotique des valeurs propres. *Nouvelles de la Société*

des Sciences sur Göttingen, Mathematical-Physical Class 110-117.

WOLFE, P. J. and OLHEDE, S. C. (2013). Nonparametric graphon estimation. *arXiv preprint arXiv:1309.5936*.

YANG, J., HAN, C. and AIROLDI, E. (2014). Nonparametric estimation and testing of exchangeable graph models. In *Artificial Intelligence and Statistics* 1060–1067.

YOUNG, S. J. and SCHEINERMAN, E. R. (2007). Random dot product graph models for social networks. In *International Workshop on Algorithms and Models for the Web-Graph* 138–149. Springer.

ZACHARY, W. W. (1977). An information flow model for conflict and fission in small groups. *Journal of anthropological research* **33** 452–473.